

Block Shear of Bolted Connections—Reliability Analysis and Design Recommendations

BO DOWSWELL

ABSTRACT

In this paper, the existing data from previous research projects was analyzed to determine the reliability of the 2022 AISC *Specification* block shear equations. Additionally, the 1989 AISC *Specification* provisions and the design equations proposed by Driver et al. (2006), Kamtekar (2012), and Teh and Deierlein (2017) were analyzed. The analysis was limited to normal-strength steels. The data set included a total of 279 experimental tests from 25 research projects. For the data set with only U-shaped block shear patterns, the reliability analysis showed that both the 2022 AISC *Specification* and the 1989 AISC *Specification* block shear provisions are conservative.

Based on the results, revisions to the AISC *Specification* were proposed. The proposed design method combines attributes from the available design methods to develop a general design method that is applicable to several common connection types. A secondary intention is to enhance clarity and transparency, where the variables affecting the strength are included explicitly in the equations.

Keywords: block shear, tensile rupture.

INTRODUCTION

Block shear occurs when a connecting element fails around the perimeter of a fastener group as shown in Figure 1. The failure pattern is characterized by tensile rupture at a plane perpendicular to the load and shear failure along either one or two planes parallel to the load.

The analysis by Galambos was used to determine the reliability of the block shear equations that were proposed for the draft of the first AISC LRFD *Specification*

for *Structural Steel Buildings*, hereafter referred to as the AISC *Specification* (1986). After the Galambos report was published, several research projects have significantly expanded the experimental data set for the block shear failure mode. Although the Commentary to 2022 AISC *Specification* Section J4.3 states that the adopted block shear model is conservative, the reliability has not been analyzed using the complete data set.

The objective of this paper is to analyze the existing data from previous research projects to determine the reliability of the 2022 AISC *Specification* block shear equations. Additionally, the 1989 AISC *Specification* provisions and the design equations proposed by Driver et al. (2006), Kamtekar (2012), and Teh and Deierlein (2017) are analyzed. Based on these results, revisions to the AISC *Specification* are proposed.

Bo Dowswell, PE, PhD, Principal, ARC International, LLC, Birmingham, Ala.
Email: bo@arcstructural.com

Paper No. 2024-12

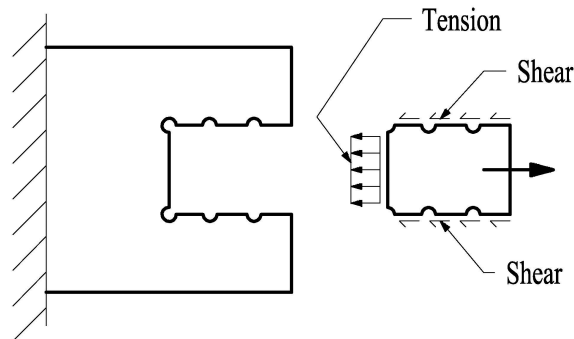


Fig. 1. Block shear.

AISC SPECIFICATION

In this section, the 2022 AISC *Specification* equations are presented, and relevant older AISC *Specification* requirements are reviewed. Detailed historical reviews were provided by Epstein and Aleksiewicz (2008) and Geschwinder (2006). Based on the test results of Birkemoe and Gilmor (1978), block shear provisions first appeared in the 1978 AISC *Specification*. Since then, the *Specification* equations changed several times.

The early equations were presented in either ASD or LRFD format with the safety and resistance factors embedded in the equations. However, these equations will be presented in this paper as nominal strengths. Because the safety factors and resistance factors have remained unchanged, using the nominal strength equations results in the most direct comparisons between the various *Specification* requirements. Because the variable symbols have changed, all equations will use the symbols defined in the 2022 AISC *Specification*.

1986 AISC Specification

The 1986 AISC *Specification* was the first LRFD specification. The block shear provisions are in Section J4.2.c. Based on the *Specification* verbiage, the block shear strength is the maximum of the two values calculated with Commentary Equations C-J4-1 and C-J4-2. Equations 1a and 1b show the nominal strengths for these equations.

$$R_n = 0.6F_y A_{gv} + F_u A_{nt} \quad (1a)$$

$$R_n = 0.6F_u A_{nv} + F_y A_{gt} \quad (1b)$$

where

A_{gv} = gross area subjected to shear, in.²

A_{gt} = gross area subjected to tension, in.²

A_{nv} = net area subjected to shear, in.²

A_{nt} = net area subjected to tension, in.²

F_u = specified minimum tensile strength, ksi

F_y = specified minimum yield stress, ksi

Galambos (1985) indicated that the draft version of the *Specification* dated 1985 had slightly different block shear equations. His analysis included a nonuniform stress factor, U_{bs} , that was originally proposed by Ricles and Yura (1983). The nonuniform stress factor was applied only to the tension planes as indicated in Equations 2a and 2b. In the draft *Specification*, the block shear strength is the minimum of the two values calculated with Equations 2a and 2b.

$$R_n = 0.6F_y A_{gv} + U_{bs} F_u A_{nt} \quad (2a)$$

$$R_n = 0.6F_u A_{nv} + U_{bs} F_y A_{gt} \quad (2b)$$

Galambos (1985) determined the reliability index for the draft *Specification* to be 3.3 when $\phi = 0.75$ and the live-to-dead-load ratio is $L/D = 3.0$. These results were based on a professional factor that was calculated using the results of 42 experimental tests from four research projects: Birkemoe and Gilmor (1978), Yura et al. (1982), Ricles and Yura (1983), and Hardash and Bjorhovde (1985).

1989 AISC Specification

The 1989 AISC *Specification* block shear provisions are in ASD format. Combining Equations J4-1 and J4-2 in Section J4 results in the equation in the Commentary to the 1978 AISC *Specification*. Multiplying by a safety factor of 2.0 results in the nominal block shear strength of Equation 3.

$$R_n = F_u A_{nt} + 0.6F_u A_{nv} \quad (3)$$

2022 AISC Specification

In the 2022 AISC *Specification*, the block shear strength is calculated with Equation J4-5, which was first included in the 2005 AISC *Specification*.

$$R_n = 0.6F_u A_{nv} + U_{bs} F_u A_{nt} \leq 0.6F_y A_{gv} + U_{bs} F_u A_{nt} \quad (\text{Spec. Eq. J4-5})$$

where

U_{bs} = nonuniform stress factor

$\Omega = 2.00$ (ASD)

$\phi = 0.75$ (LRFD)

Where the tension stress is uniform, $U_{bs} = 1$; where the tension stress is nonuniform, $U_{bs} = 0.5$. Commentary Figure C-J4.2 indicates that $U_{bs} = 0.5$ for beam shear connections with multiple vertical bolt rows and $U_{bs} = 1$ for all other conditions. The nonuniform stress factor of 0.5 was first recommended by Ricles and Yura (1983), based on the reduced block shear strength and nonlinear stress distribution at the tension plane of bolted clip angle connections with two vertical bolt rows. Although U_{bs} was not included in the 1989 *Specification* block shear provisions, the 50% strength reduction on the tension plane was widely used in practice because it was discussed in *Engineering for Steel Construction* (AISC, 1984) and the *Manual of Steel Construction—Volume II—Connections* (AISC, 1992).

BACKGROUND

This section of the paper provides background information on the *Specification* provisions. It is not intended to provide a complete review of the available research.

Tests by Chesson and Munse (1958, 1963) revealed a limit state with failure around the periphery of fastener (rivets and bolts) groups connecting axially loaded members to gusset plates. Birkemoe and Gilmor (1978) showed experimentally that block shear failure can occur in coped beams with bolted clip angle connections as shown in the L-shaped pattern of Figure 2(a). Marsh (1979) tested 43 bolted double-lap gusset plate connections of steel and aluminum. Marsh was the first to propose a design equation for the U-shaped pattern shown in Figure 2(b). Both the Birkemoe/Gilmor and Marsh research indicated that the block shear strength can be accurately predicted by summing the net rupture strengths of the tension and shear planes.

Tests on 28 bolted gusset plates by Hardash and Bjorhovde (1984, 1985) showed that the limit state is defined by rupture across the tension plane, with various levels of yielding along the shear planes. The extent of shear yielding was dependent on the length of the shear plane. The researchers proposed an empirical equation for the effective shear stress, which varies between the shear yield stress and the shear rupture stresses.

Cunningham et al. (1995) summarized the available test data and concluded that the aspect ratio of the block may have a significant effect on the strength. In cases where the resistance is not symmetrical about the loading plane, the in-plane eccentricity reduces the block shear strength. They noted that the strength can be accurately predicted by summing the net rupture strength of the tension plane and the gross yield strength of the shear planes. Kulak and Grondin (2001) summarized the available test data on gusset plates and came to the same conclusion.

Tests analyzed by Cunningham et al. (1995) and Kulak and Grondin (2001) showed that failure loads of coped beams decrease when the load is applied with an

eccentricity relative to the shear failure plane [Figure 3(a)]. This is because the tensile stresses are nonuniform. The triangular stress distribution shown in Figure 3(b) was first recommended by Ricles and Yura (1983) based on their experimental tests.

OTHER DESIGN METHODS

The design methods proposed by Driver et al. (2006), Kamtekar (2012), and Teh and Deierlein (2017) are discussed in this section of the paper.

Driver et al. (2006)

Huns et al. (2002) and Driver et al. (2006) showed that the block shear failure mode consists of shear yielding on the gross section adjacent to the holes, combined with rupture on the net tension area. They proposed Equation 4, where the strength is calculated by combining the net rupture strength of the tension plane with the strength of the shear planes. The shear plane strength is calculated with an effective shear stress, which is the average of the yield and rupture shear stress, applied to the gross shear area.

$$R_n = U_t A_{nt} F_u + 0.6 U_v A_{gv} \left(\frac{F_y + F_u}{2} \right) \quad (4)$$

where

- U_t = nonuniform tension stress factor
- U_v = nonuniform shear stress factor

For gusset plates with a U-shaped pattern, as shown in Figure 2(b), $U_t = 1$ and $U_v = 1$. When used with a reduction factor of $\phi = 0.75$, This results in a reliability index, β , of 4.4 (Huns et al., 2002). For angles and tees, $U_t = 0.9$ and $U_v = 0.9$. For beam end connections with a single vertical row of bolts, as shown in Figure 2(a), $U_t = 0.9$ and $U_v = 1$. For beam

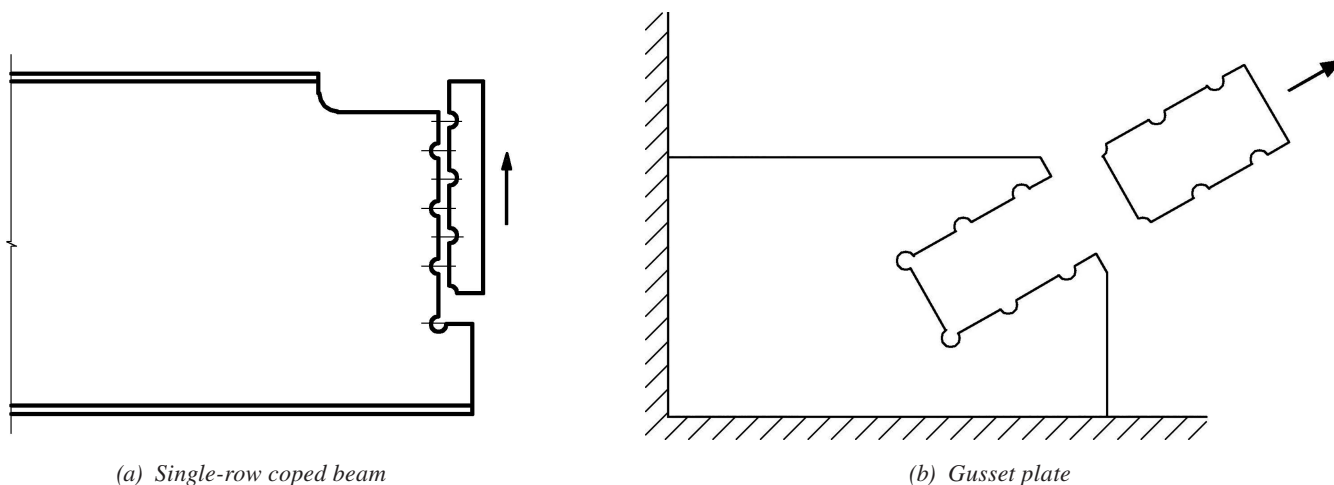


Fig. 2. Block shear with uniform tension stress.

Table 1. Nonuniform Tension and Shear Stress Factors		
	U_t	U_v
Gusset plates	1	1
Angles and tee webs	0.9	0.9
Coped beam with one vertical bolt row	0.9	1
Coped beam with two vertical bolt rows	0.3	1

Table 2. Nonuniform Tension Stress Factors, U_t	
Gusset plates	1
Angles and tee webs	0.6
Coped beam with one vertical bolt row	0.9
Coped beam with two vertical bolt rows	0.3

end connections with two vertical rows, as shown in Figure 3(a), $U_t = 0.3$ and $U_v = 1$. The recommended coefficients are summarized in Table 1.

Driver et al. (2006) modified Equation 4 by deleting U_v and recalibrating U_t . This resulted in Equation 5, which is used with the nonuniform tension stress factors in Table 2. Equation 5 was adopted in the Canadian standard, CAN/CSA-S16-14 *Design of Steel Structures* (2014). When used with a resistance factor of $\phi = 0.75$, the resulting reliability index is 4.3 for gusset plates and 3.5 for angles, tee webs, and coped beams. Driver et al. noted that reliability indices less than 4 may be appropriate for the block shear limit state because the ductility is significantly higher than for bolts and welds.

$$R_n = U_t A_{nt} F_u + 0.6 A_{gv} \left(\frac{F_y + F_u}{2} \right) \quad (5)$$

Kamtekar (2012)

The research by Kamtekar (2012) was primarily related to bolt tearout. The tearout strength is calculated using two shear rupture planes between the bolt hole and the member edge. The shear planes are located at the bolt edge, and the shear plane length is calculated using the geometry of the connection (edge distance, bolt diameter, and hole diameter). The same concept was also proposed for the block shear limit state, where the shear area is calculated at the bolt edge as shown in Figure 4.

The block shear strength is calculated with Equation 6.

$$R_n = F_u A_{nt} + 0.6 F_u A_{ev} \quad (6)$$

For connections with round holes, A_{ev} is calculated with a shear length reduction for each hole in the shear plane, l_{vh} , according to Equation 7.

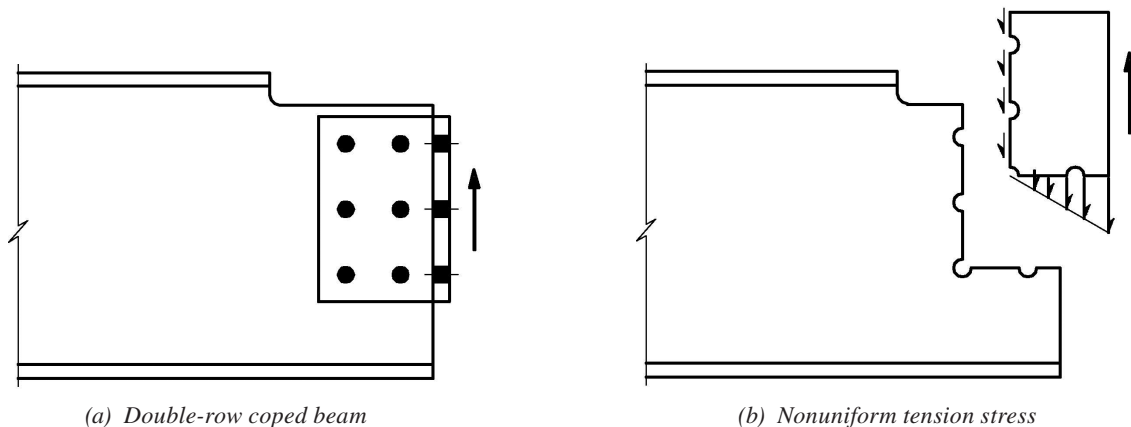


Fig. 3. Block shear of a double-row coped beam web.

$$l_{vh} = \sqrt{d_h^2 - d^2} \quad (7)$$

where

- A_{ev} = effective shear area, in.²
- d = bolt diameter, in.
- d_h = hole diameter, in.

Teh and Deierlein (2017)

The design method proposed by Teh and Deierlein (2017) is based on an effective shear area equal to the average of the gross and net shear areas. The block shear strength is calculated using Equation 6 with the effective shear area calculated with Equation 8.

$$A_{ev} = \frac{A_{gv} + A_{nv}}{2} \quad (8)$$

STATISTICAL PARAMETERS

The objective of this section of the paper is to analyze the existing data from previous research projects. An accurate reliability analysis must consider the actual, measured geometries and material strengths. The bias and variation between actual and specified properties are discussed. The bias coefficient is:

$$\rho_R = \rho_M \rho_G \rho_P \quad (9)$$

where

- ρ_G = bias coefficient for the geometric properties, addressing the difference between the nominal and actual dimensions
- ρ_M = bias coefficient for the material properties, addressing the difference between the specified and actual strengths
- ρ_P = bias coefficient for the test-to-predicted strength ratios; mean value of the professional factor calculated with the measured geometric and material properties

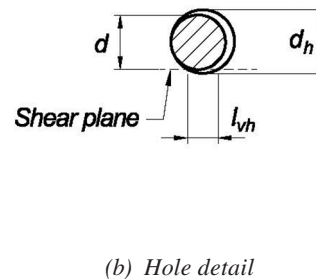
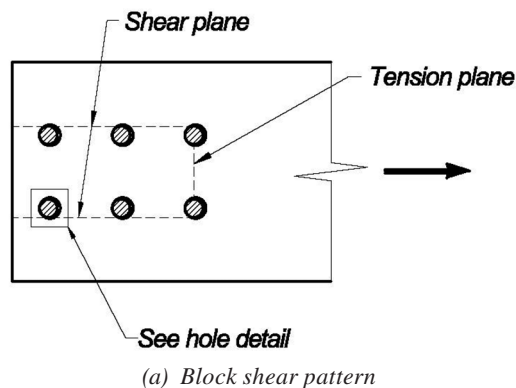


Fig. 4. Kamtekar (2012) block shear pattern.

The coefficient of variation is:

$$V_R = \sqrt{V_M^2 + V_G^2 + V_P^2} \quad (10)$$

where

- V_G = coefficient of variation for the geometric properties
- V_M = coefficient of variation for the material properties
- V_P = coefficient of variation for the test-to-predicted strength ratios

Geometric Properties

For the block shear limit state, geometric variations are primarily related to the element thickness. For plate thickness variation, Hess et al. (2002) recommended $\rho_G = 1.05$ with $V_G = 0.044$, and Schmidt and Bartlett (2002) recommended $\rho_G = 1.04$ with $V_G = 0.025$. The values for W-shape webs from Franchuk et al. (2004) are $\rho_G = 1.017$ with $V_G = 0.039$.

Due to a lack of statistical data associated with the effect of fabrication tolerances (hole size, spacing, edge distance) on block shear strength, these variabilities are usually included implicitly in first-order reliability analyses. To consider the effect of geometric variations, including fabrication tolerances, Galambos and Ravinda (1978) recommended $\rho_G = 1.00$ with $V_G = 0.050$. These values, which were used in the block shear reliability analysis by Hardash and Bjorhovde (1984), were also used in this paper.

Material Properties

Recommended statistical parameters for the material tensile strength were summarized by Schmidt and Bartlett (2002). For plates with thicknesses between 10 mm (0.39 in.) and 20 mm (0.79 in.), $\rho_M = 1.19$ with $V_M = 0.034$. These values are conservative compared to those of thicker plates. For I-shaped members, $\rho_M = 1.13$ with $V_M = 0.044$.

Liu et al. (2007) compiled the following tensile strength data:

- For ASTM A992 (2022) W-shapes, $\rho_M = 1.12$ with $V_M = 0.04$. These values are conservative for ASTM A36 (2019a) and ASTM A572 (2021) Grade 50 W-shapes.
- For A572 Grade 50 angles, $\rho_M = 1.38$ with $V_M = 0.06$. The worst case is for A36 angles, where $\rho_M = 1.22$ with $V_M = 0.04$.
- For A36 channels, $\rho_M = 1.18$ with $V_M = 0.04$. However, the preferred material specification in AISC *Manual* (AISC, 2023) Table 2-4 is A992.
- The mean values for ASTM A529 (2019b) and A572 plates are $\rho_M = 1.21$ with $V_M = 0.04$. The worst case is for A572 Grade 55 plates, where $\rho_M = 1.15$ with $V_M = 0.01$.

Recommended statistical parameters for the material yield strength were summarized by Schmidt and Bartlett (2002). For plates with thicknesses between 10 mm (0.39 in.) and 20 mm (0.79 in.), $\rho_M = 1.11$ with $V_M = 0.054$. These values are conservative for thicker plates. For I-shaped members, $\rho_M = 1.03$ with $V_M = 0.063$.

Liu et al. (2007) compiled the following yield strength data:

- For A992 W-shapes, $\rho_M = 1.10$ with $V_M = 0.05$. These values are conservative for A36 and A572 Grade 50 W-shapes.
- For A572 Grade 50 angles, $\rho_M = 1.29$ with $V_M = 0.07$. These values are conservative for A36 and ASTM A588 (2024) angles.
- For A36 channels, $\rho_M = 1.36$ with $V_M = 0.06$. However, the preferred material specification in AISC *Manual* Table 2-4 is A992.
- The mean values for A529 and A572 plates are $\rho_M = 1.15$ with $V_M = 0.06$. The worst case is for A529 Grade 55 plates, where $\rho_M = 1.10$ with $V_M = 0.05$.

Block shear is a valid limit state for each of the available shapes. Although the shear plane strength in 2022 AISC *Specification* Equation J4-5 is limited by the yield strength, the research discussed in this paper indicates that the block shear strength is more accurately predicted with the tensile strength on both the tension and shear planes. Therefore, the lower-bound bias coefficient for tensile strength, $\rho_M = 1.12$, was used in the analysis with $V_M = 0.044$.

Test-to-Predicted Strength

The bias coefficient and coefficient of variation for the test-to-predicted strength ratios, ρ_P and V_P are discussed in this section of the report. These statistical parameters were calculated using existing data from previous research

projects. Only specimens with quasi-static loading were included in the data set. The specimens had measured yield stresses between 33.2 and 79.8 ksi. The measured tensile strengths were between 46.8 and 89.3 ksi.

Table 3 provides a summary of the specimens. The data set included a total of 279 experimental tests from 25 research projects. The third column of Table 3 lists the failure pattern that was observed for each specimen.

The test-to-predicted strength parameters are listed in Table 4. Because the various specimen characteristics result in different eccentricities and failure patterns, an evaluation of each connection type is required. Some of the connection types require a nonuniform stress factor; however, these were not included in the Table 4 values. Therefore, only the groups without eccentricity are expected to be accurate. For the other cases, the statistical parameters will be used to determine nonuniform stress factors that result in the lowest V_P values and an appropriate reliability index. Single-row and double-row terminology refers to the number of bolt rows parallel to the loading direction.

RELIABILITY ANALYSIS

In this section of the paper, the statistical parameters are used to determine the reliability of block shear equations from the 2022 AISC *Specification*, the 1989 AISC *Specification*, Driver et al. (2006), Kamtekar (2012), and Teh and Deierlein (2017). The resistance factor required to obtain a specific reliability level is (Galambos and Ravinda, 1978)

$$\phi = C_R \rho_R e^{-\beta \alpha_R V_R} \quad (11)$$

where

C_R = load ratio correction factor

V_R = coefficient of variation

α_R = separation factor

β = reliability index

ρ_R = bias coefficient

Galambos and Ravinda (1973) recommended a separation factor, α_R , of 0.55. For $L/D = 3.0$, Li et al. (2007) developed Equation 12 for calculating the load ratio correction factor.

$$C_R = 1.40 - 0.156\beta + 0.0078\beta^2 \quad (12)$$

The bias coefficient and the coefficient of variation are calculated using the statistical parameters with Equations 9 and 10, respectively. Equations 9 through 12 are accurate only for large sample sizes; however, many of the data sets consist of only a limited number of tests. To consider the effect of small sample sizes, AISI (2016) uses a correction factor applied to V_P , resulting in a coefficient of variation of

$$V_R = \sqrt{V_M^2 + V_G^2 + C_p V_P^2} \quad (13)$$

Table 3. Experimental Tests			
Reference	Element	Failure Pattern	<i>n</i>
Gusset Plates			
Chesson and Munse (1958)	Shaped gusset plate	U	2
Chesson and Munse (1963)	Shaped gusset plate	U	8
Hardash and Bjorhovde (1984)	Rectangular plate	U	28
Udagawa and Yamada (1998)	Rectangular plate	U	49
Huns et al. (2002)	Rectangular plate	U	5
Mullin and Cheng (2004)	Shaped gusset plate	U	5
Brown et al. (2007)	Rectangular plate	U	26
Zeynali et al. (2017)	Rectangular plate	U	22
Braces			
Madugula and Mohan (1988)	Angle brace	L	12
Epstein (1992)	Angle brace	L	2
Sankisa (1993)	Angle brace	L	18
Gross et al. (1995)	Angle brace	L	13
Orbison et al. (1999)	Angle brace	L	3
Orbison et al. (1999)	Web of T-shaped brace	L	9
Aalberg and Larsen (2000)	Web of I-shaped brace	U	4
Bartels (2000)	Web of T-shaped brace	L	3
Castonguay (2009)	Angle brace	L	3
McNeill and Lloyd (2018)	Web of C-shaped brace	U	1
McNeill and Lloyd (2018)	Angle brace	L	1
Pizzuto (2019)	Flange of I-shaped brace	L	7
Jiang et al. (2020)	Angle brace	L	11
Ke et al. (2022)	Angle brace	L	5
Ke et al. (2022)	Angle brace	U	1
Beams			
Birkemoe and Gilmor (1978)	Coped beam	L	1
Yura et al. (1982)	Coped beam	L	4
Ricles and Yura (1983)	Coped beam	L	7
Aalberg and Larsen (2000)	Coped beam	L	8
Franchuk et al. (2004)	Coped beam	L	15
Fang et al. (2013)	Coped beam	L	10
<i>n</i> = sample size			

Table 4. Test-to-Predicted Strength Parameters

	AISC Specification (2022)	AISC Specification (1989)	Driver et al. (2006)	Kamtekar (2012)	Teh and Deierlein (2017)
All Specimens (n = 279)					
ρ_P	1.16	1.15	1.03	0.952	0.986
V_P	0.113	0.119	0.138	0.115	0.111
Specimens with U-Shaped Failure Pattern (n = 151)					
ρ_P	1.20	1.19	0.995	1.00	1.02
V_P	0.0755	0.0790	0.0801	0.0675	0.0682
Single-Row Brace (n = 72)					
ρ_P	1.07	1.07	0.988	0.888	0.913
V_P	0.128	0.129	0.204	0.128	0.127
Double-Row Brace (n = 8)					
ρ_P	1.02	1.02	1.17	0.918	0.907
V_P	0.0860	0.0919	0.177	0.0872	0.0835
Single-Row Beam (n = 26)					
ρ_P	1.17	1.14	0.965	0.948	0.980
V_P	0.0885	0.102	0.0756	0.0947	0.0945
Double-Row Beam (n = 15)					
ρ_P	0.885	0.829	0.784	0.760	0.769
V_P	0.167	0.216	0.169	0.197	0.203
<i>n</i> = sample size					

The sample size correction factor for $n \geq 4$ is

$$C_P = \left(1 + \frac{1}{n}\right) \left(\frac{m}{m-2}\right) \quad (14)$$

$$= \left(1 + \frac{1}{n}\right) \left(\frac{n-1}{n-3}\right)$$

where

m = degrees of freedom

= $n - 1$

n = number of tests

Equation 14 was originally developed by Hall and Pekoz (1988) and revised by Tsai (1992).

Based on the 2022 AISC *Specification* Section B3.1 Commentary, the primary target reliability index used in this report is 4.0. The use of $\beta = 4.0$ for the block shear limit state is discussed further by Franchuk et al. (2004), Teh and Deierlein (2017), and Yam et al. (2011).

Results

The accuracy of the basic equation, without a nonuniform stress factor, is established using only the data set with a

U-shaped failure pattern. This data set includes gusset plates, double-row angle braces, I-shaped brace webs, and a channel brace web. The resistance factors calculated with Equation 11 are listed in Table 5. These values were determined with $C_p = 1.02$, which was calculated using Equation 14 with $n = 151$.

For connections with a U-shaped failure pattern, $\phi = 0.95$ results in an appropriate reliability level for the AISC (2022, 1989) equations. For the Driver et al. (2006), Kamtekar (2012), and Teh and Deierlein (2017) equations, $\phi = 0.80$ is appropriate.

ANALYSIS AND DISCUSSION

In this section of the paper, further analysis of the published research is used to establish the effect of oversize holes, shear plane location and the nonuniform stress factor on the block shear strength.

Oversize Holes

Three specimens with oversize holes were tested by Har-dash and Bjorhovde (1984). All three specimens had

	AISC Specification (2022)	AISC Specification (1989)	Driver et al. (2006)	Kamtekar (2012)	Teh and Deierlein (2017)
ϕ	0.968	0.954	0.796	0.817	0.833

Specimen	AISC Specification (2022)	AISC Specification (1989)	Driver et al. (2006)	Kamtekar (2012)	Teh and Deierlein (2017)
16	1.21	1.21	0.999	1.08	1.01
20	1.28	1.28	1.08	1.16	1.09
26	1.26	1.26	1.03	1.12	1.05
Mean	1.25	1.25	1.04	1.12	1.05

U-shaped failure patterns. For these specimens, which had 1/2-in.-diameter bolts with 1/16-in.-diameter holes, the test-to-predicted strength ratios are listed in Table 6. The last row shows the mean values, which are higher than the ρ_P values for the specimens with U-shaped failure pattern in Table 4 for all five design equations. The ratios of the mean value from Table 6 to the ρ_P values from Table 4 vary from 1.03 to 1.12, with the Teh and Deierlein equation resulting in the smallest ratio.

Shear Plane Location

Based on the Birkemoe and Gilmor (1978) recommendations, the net tensile and shear areas have traditionally been calculated along the hole centers. However, Kamtekar (2012) and Teh and Deierlein (2017) showed that, for bolted gusset plate connections, the shear failure plane is located between the center and edge of the holes, resulting in increased shear plane areas.

For connections that are symmetrical about the loading axis, bearing of the bolts on the holes induces a secondary constraining force perpendicular to the load (Wen and Mahmoud, 2017), resulting in the shear plane locations shown earlier in Figure 4. Where this constraint is not available, lateral translation of the block causes the shear

plane to shift closer to the hole center, as shown in Figure 5. This effect causes a reduction in the shear plane area when compared to constrained elements. The differences in constrained and unconstrained behavior can be clearly identified in many of the post-test photographs in the references of Table 3.

For constrained connections, the Kamtekar (2012) and Teh and Deierlein (2017) equations result in similar reliabilities, with the Kamtekar equation marginally more accurate based on the parameters for U-shaped failure patterns in Table 4. The Kamtekar equation is based on a theoretical failure mechanism and the Teh and Deierlein equation appears to be an empirical estimate. Due to the lack of significant experimental specimens with oversize holes, an accurate reliability assessment of the two equations for this condition is not available. However, the three data points in Table 6 show that both equations are conservative for this limited data set.

To isolate the shear plane in a U-shaped block shear pattern, Orbison et al. (1999) and Aalberg and Larsen (2000) tested I-shaped brace web specimens with the tension plane cut. The test-to-predicted strength parameters for the test by Aalberg and Larsen and five tests by Orbison et al. are listed in Table 7. Based on the ρ_P and V_P values for the five

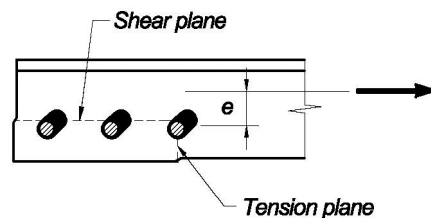


Fig. 5. Nonconstrained connection.

Table 7. Test-to-Predicted Strength Parameters for Shear-Plane Specimens					
	AISC Specification (2022)	AISC Specification (1989)	Driver et al. (2006)	Kamtekar (2012)	Teh and Deierlein (2017)
Aalberg and Larsen (2000) Test					
Specimen T4-1	1.46	1.46	1.11	1.06	1.14
Orbison et al. (1999) Tests					
Specimen W3	1.27	1.27	1.02	1.00	1.04
Specimen W7	1.31	1.31	1.02	1.01	1.06
Specimen W8	1.25	1.25	0.991	0.978	1.02
Specimen W9	1.25	1.25	1.05	1.02	1.05
Specimen W10	1.17	1.17	0.981	0.952	0.987
Reliability Parameters					
ρ_P	1.29	1.29	1.03	1.00	1.05
V_P	0.0678	0.0678	0.0404	0.0331	0.0471
ϕ	1.01	1.01	0.857	0.843	0.861

block shear equations, the Kamtekar equation is clearly the most accurate.

The tearout limit state for bolted connections occurs when a shear plane rupture occurs parallel to the load on each side of the bolt. The tearout limit state is similar to the block shear limit state without the tension rupture plane. Because there are a significant number of experimental tests available for the tearout limit state, further insight into the behavior of isolated shear planes can be gained by observing these results, which were analyzed by Franceschetti and Denavit (2021). Franceschetti and Denavit indicated that the two effective area methods (Kamtekar, 2012; Teh and Deierlein, 2017) are more accurate than the net area method (AISC, 1989, 2022). They recommended the equation by Kamtekar because it “showed less variation” than the Teh and Deierlein equation and “was found to be accurate over the entire range of hole types investigated.”

Nonuniform Stress Factor

Based on the Ricles and Yura (1983) recommendations, the nonuniform stress factor has traditionally been applied to the tension plane resistance. In this study, the accuracy of the nonuniform stress factor was investigated iteratively as a multiplier on the tension term, on the shear term, and to both the tension and shear terms. These comparisons resulted in a minimum coefficient of variation when the nonuniform stress factor was applied to the shear plane resistance. This is because, under some conditions, the block shear strength can be limited by tension plane rupture with a relatively low shear plane efficiency (Cunningham et al. 1995; Orbison et al., 1999; Wen and Mahmoud, 2017).

PROPOSED DESIGN METHOD

Because Equation 3 is simple, transparent, and accurate for many different design conditions, it was used as the basis for the proposed design method. The effective shear area is used in lieu of the net area to allow the use of increased shear areas for laterally constrained elements. A shear plane efficiency factor is used to consider the effect of eccentricity on the shear plane resistance. The nominal strength for the limit state of block shear is

$$R_n = F_u(A_{nt} + 0.6U_vA_{ev}) \quad (15)$$

where

U_v = shear plane efficiency factor

Ω = 1.88 (ASD)

ϕ = 0.80 (LRFD)

Effective Shear Area

For block shear patterns that are symmetrical about the loading axis as shown in Figure 6, the effect of lateral constraint on the shear area can be calculated with an effective hole diameter. For connections with round holes, A_{ev} is calculated with a shear length reduction for each hole in the shear plane, l_{vh} , according to Equation 7. For connections with slotted holes, l_{vh} is the slot dimension parallel to the shear plane. For block shear patterns that are unsymmetrical about the loading axis as shown in Figure 7, A_{ev} should be calculated with the actual hole diameter, d_h . For both symmetrical and unsymmetrical block shear patterns, the net areas should be calculated according to 2022 AISC Specification Section B4.3b, which requires “the

Table 8. Reliability Parameters for Eccentric Specimens					
	U_v	n	ρ_P	V_P	ϕ
Single-row brace	1.0	72	1.07	0.129	0.779
Double-row brace	0.90	8	1.06	0.0898	0.818
Single-row beam	1.0	26	1.14	0.102	0.869
Double-row beam	0.30	15	1.26	0.177	0.803

$n =$ sample size

width of a bolt hole shall be taken as $\frac{1}{16}$ in. (2 mm) greater than the nominal dimension of the hole.”

Eccentricity

The shear plane efficiency factor is used to consider the effect of eccentricity on the shear plane resistance. For the concentrically loaded patterns shown in Figure 6, $U_v = 1.0$. For the eccentrically loaded patterns shown in Figure 7, a reliability analysis is used to calculate the values for U_v to result in $\beta \approx 4$ when $\phi = 0.80$. Table 8 lists the reliability

parameters for each connection type. Here, ρ_P and V_P were calculated with Equation 15. The recommended U_v factors are listed in the second column.

CONCLUSIONS

In this paper, the existing data from previous research projects was analyzed to determine the reliability of the 2022 AISC *Specification* block shear equations. Additionally, the 1989 AISC *Specification* provisions and the design equations proposed by Driver et al. (2006), Kamtekar (2012),

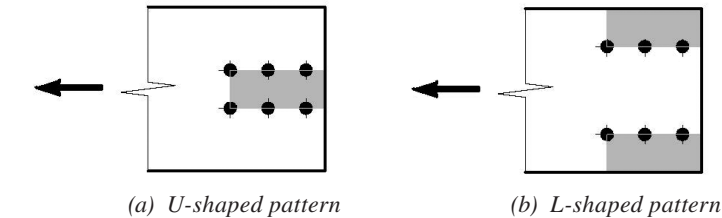


Fig. 6. Symmetrical block shear patterns.

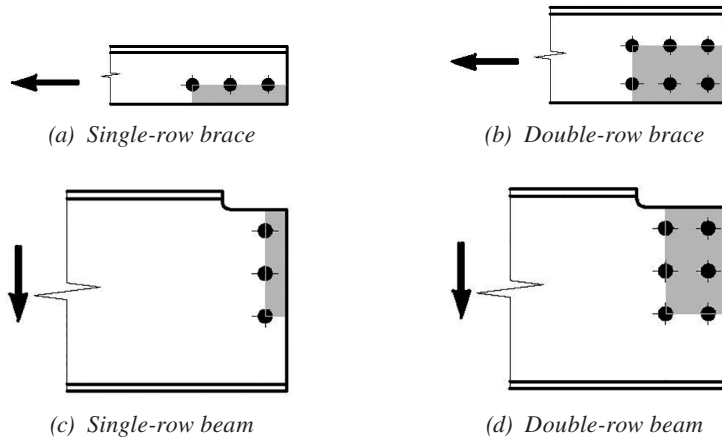


Fig. 7. Unsymmetrical block shear patterns.

and Teh and Deierlein (2017) were analyzed. The analysis was limited to normal strength steels. The data set included a total of 279 experimental tests from 25 research projects. Based on the results, revisions to the AISC *Specification* were proposed.

For the data set with only U-shaped block shear patterns, the reliability analysis showed that both the 2022 AISC *Specification* and the 1989 AISC *Specification* block shear provisions are conservative. Although the 2022 AISC *Specification* requires $\phi = 0.75$, the analysis showed that $\phi = 0.968$ provides an appropriate reliability level. The 1989 AISC *Specification* requires $\Omega = 2.00$; however, $\Omega = 1.50/0.954 = 1.55$ results in adequate reliability. For the Driver et al. (2006), Kamtekar (2012), and Teh and Deierlein (2017) equations, $\phi = 0.80$ is appropriate.

When the data set was expanded to include both U-shaped and L-shaped block shear patterns, the coefficient of variation increased for all five of the design methods that were included in the analysis. This increase is attributed to the effects of lateral constraint and eccentricity, which were considered differently in the various design models.

The proposed design method combines attributes from the available design methods to develop a general design method that is applicable to several common connection types. A secondary intention is to enhance clarity and transparency, where the variables affecting the strength are included explicitly in the equations.

To accurately account for the behavior at failure, F_u is always used to calculate the shear plane strength. This increases the accuracy, simplifies the design equation and eliminates a source of conservatism in the 2022 AISC *Specification* equations.

One source of conservatism in the 2022 AISC *Specification* provisions is the assumption that shear failure occurs along the hole center. That is typically the case for the unsymmetrical (nonconstrained) L-shaped block shear patterns. However, for symmetrical (constrained) U-shaped and L-shaped failure patterns, the shear plane location along the bolt edge increases the shear area. It was concluded that lateral constraint, which is not present at the unsymmetrical L-shaped patterns, is required to cause the shear plane to shift from the hole center to the bolt edge. For nonconstrained connections, the proposed design method is based on the shear area along the hole center. For constrained connections, the shear area along the bolt edge is used. The proposed equations closely model the true location of the shear failure planes for both U- and L-shaped failure patterns.

The block shear strength is also dependent on the loading eccentricity, which is considered with a nonuniform stress factor. In the 2022 AISC *Specification*, the nonuniform stress factor is applied to the tension plane resistance. However, the block shear equations are more accurate when

the nonuniform stress factor is applied to the shear plane resistance. A separate reliability analysis was used to calculate these shear plane efficiency factors for four common connection types.

For the proposed design method, the reliability analysis resulted in an appropriate reliability level when $\phi = 0.80$. Compared to the 2022 AISC *Specification* provisions, the proposed design method results in a mean 24% increase in the available strength for connections with U-shaped failure patterns.

REFERENCES

- Aalberg, A. and Larsen, P.K. (2000), "Strength and Ductility of Bolted Connections in Normal and High Strength Steels," *Structural Failure and Plasticity*, Proceedings of IMPLAST 2000, Elsevier, pp. 487–494.
- AISC (1978), *Specification for the Design, Fabrication and Erection of Structural Steel for Buildings*, American Institute of Steel Construction, Chicago, Ill.
- AISC (1984), *Engineering for Steel Construction*, American Institute of Steel Construction, Chicago, Ill.
- AISC (1986), *Load and Resistance Factor Design Specification for Structural Steel Buildings*, American Institute of Steel Construction, Chicago, Ill.
- AISC (1989), *Specification for Structural Steel Buildings*, American Institute of Steel Construction, Chicago, Ill.
- AISC (1992), *Manual of Steel Construction—Volume II—Connections*, American Institute of Steel Construction, Chicago, Ill.
- AISC (2005), *Specification for Structural Steel Buildings*, ANSI/AISC 360-05, American Institute of Steel Construction, Chicago, Ill.
- AISC (2022), *Specification for Structural Steel Buildings*, ANSI/AISC 360-22, American Institute of Steel Construction, Chicago, Ill.
- AISC (2023), *Steel Construction Manual*, 16th Ed., American Institute of Steel Construction, Chicago, Ill.
- AISI (2016), *North American Specification for the Design of Cold-Formed Steel Structural Members*, American Iron and Steel Institute, Washington, D.C.
- ASTM (2019a), *Standard Specification for Carbon Structural Steel*, ASTM A36/36M, ASTM International, West Conshohocken, Pa.
- ASTM (2019b), *Standard Specification for High-Strength Carbon-Manganese Steel of Structural Quality*, ASTM A529/529M, ASTM International, West Conshohocken, Pa.

- ASTM (2021), *Standard Specification for High-Strength Low-Alloy Columbium-Vanadium Structural Steel*, ASTM A572/572M-21e1, ASTM International, West Conshohocken, Pa.
- ASTM (2022), *Standard Specification for Structural Steel Shapes*, ASTM A992/992M, ASTM International, West Conshohocken, Pa.
- ASTM (2024), *Standard Specification for High-Strength Low-Alloy Structural Steel, Up to 50 ksi [345 MPa] Minimum Yield Point, with Atmospheric Corrosion Resistance*, ASTM A588/588M, ASTM International, West Conshohocken, Pa.
- Bartels, P.A. (2000), “Net Section Rupture in Tension Members with Connection Eccentricity,” Master’s Thesis, West Virginia University, Morgantown, Va.
- Birkemoe, P.C. and Gilmor, M.I. (1978), “Behavior of Bearing Critical Double-Angle Beam Connections,” *Engineering Journal*, AISC, Vol. 15, No. 4, pp. 109–115.
- Brown, J.D., Lubitz, D.J., Cekov, Y.C., Frank, K.H., and Keating, P.B. (2007), “Evaluation of Influence of Hole Making Upon the Performance of Structural Steel Plates and Connections,” Report No. FHWA/TX-07/0-4624-1, The University of Texas at Austin.
- Castonguay, P.X. (2009), “Seismic Performance of Concentrically Braced Steel Frames of the Conventional Construction Category,” Master’s Thesis, Polytechnique Montréal.
- Chesson, E. and Munse, W.H. (1958), “Behavior of Riveted Truss-Type Connections,” *Transactions of the American Society of Civil Engineers*, American Society of Civil Engineers, Vol. 123, No. 1.
- Chesson, E. and Munse, W.H. (1963), “Riveted and Bolted Joints: Truss-Type Tensile Connections,” *Journal of the Structural Division*, American Society of Civil Engineers, Vol. 89, No. ST1.
- CSA (2014), *Design of Steel Structures*, Standard S16-14, Canadian Standards Association.
- Cunningham, T.J., Orbison, J.G., and Ziemian, R.D. (1995), “Assessment of American Block Shear Load Capacity Predictions,” *Journal of Constructional Steel Research*, Vol. 35.
- Driver, R.G., Grondin, G.Y., and Kulak, G.L. (2006), “Unified Block Shear Equation for Achieving Consistent Reliability,” *Journal of Constructional Steel Research*, Vol. 62.
- Epstein, H.I. (1992), “An Experimental Study of Block Shear Failure of Angles in Tension,” *Engineering Journal*, AISC, Vol. 29, No. 2, pp. 75–84.
- Epstein, H.I. and Aleksiewicz, L.J. (2008), “Block Shear Equations Revisited...Again,” *Engineering Journal*, AISC, Vol. 45, No. 1, pp. 5–12.
- Fang, C., Lam, A.C.C., Yam, M.C.H., and Seak, K.S. (2013), “Block Shear Strength of Coped Beams with Single-Sided Bolted Connection,” *Journal of Constructional Steel Research*, Vol. 86.
- Franceschetti, N. and Denavit, M.D. (2021), “Tearout Strength of Concentrically Loaded Bolted Connections,” *Engineering Journal*, AISC, Vol. 58, No. 3, pp. 165–184.
- Franchuk, C.R., Driver, R.G., and Grondin, G.Y. (2004), “Reliability Analysis of Block Shear Capacity of Coped Steel Beams,” *Journal of Structural Engineering*, ASCE, Vol. 130, No. 12, December, pp. 1904–1913.
- Galambos, T.V. (1985), “Reliability of Connections, Joints and Fasteners,” Structural Engineering Report No. 85-05, Department of Civil and Environmental Engineering, Washington University, St. Louis, Mo.
- Galambos, T.V. and Ravinda, M.K. (1973), “Tentative Load and Resistance Factor Design Criteria for Steel Buildings,” Research Report No. 18, Department of Civil and Environmental Engineering, Washington University, St. Louis, Mo.
- Galambos, T.V. and Ravinda, M.K. (1978), “Load and Resistance Factor Design for Steel,” *Journal of the Structural Division*, ASCE, Vol. 104, No. ST9.
- Geschwinder, L.F. (2006), “Evolution of Shear Lag and Block Shear Provisions in the AISC Specification,” *Engineering Journal*, AISC, Vol. 43, No. 4, pp. 237–240.
- Gross, J.M., Orbison, J.G., and Ziemian, R.D. (1995), “Block Shear Tests in High-Strength Steel Angles,” *Engineering Journal*, AISC, Vol. 32, No. 3, pp. 117–122.
- Hall, B.W. and Pekoz, T. (1988), “Probabilistic Evaluation of Test Results,” *Ninth International Specialty Conference on Cold-Formed Steel Structures*, St. Louis, Mo., November 8–9.
- Hardash, S.G. and Bjorhovde, R. (1984), *Gusset Plate Design Utilizing Block Shear Concepts*, Department of Civil Engineering and Engineering Mechanics, University of Arizona, Tucson, Az.
- Hardash, S.G. and Bjorhovde, R. (1985), “New Design Criteria for Gusset Plates in Tension,” *Engineering Journal*, AISC, Vol. 22, No. 2, pp. 77–94.
- Hess, P.E. Bruchman, D., Assakkaf, I.A., and Ayyub, B.M. (2002), “Uncertainties in Material Strength, Geometric and Load Variables,” *Naval Engineers Journal*, Vol. 114, No. 2.
- Huns, B.B.S., Grondin, G.Y., and Driver, R.G. (2002), “Block Shear Behavior of Bolted Gusset Plates,” Structural Engineering Report 248, University of Alberta, Canada.

- Jiang, D., Yam, M.C.H., Ke, K., Lam, A.C.C., and Zhao, Q. (2020), "Block Shear Failure of S275 and S690 Steel Angles with Single-Line Bolted Connections," *Journal of Constructional Steel Research*, Vol. 170.
- Kamtekar, A.G. (2012), "On the Bearing Strength of Bolts in Clearance Holes," *Journal of Constructional Steel Research*, Vol. 79.
- Ke, K., Zhang, M., Yam, M.C.H., Lam, A.C.C., Wang, J. and Jiang, B. (2022), "Block Shear Performance of Double-Line Bolted S690 Steel Angles Under Uniaxial Tension," *Thin-Walled Structures*, Vol. 171.
- Kulak, G.L. and Grondin, G.Y. (2001), "AISC LRFD Rules for Block Shear in Bolted Connections—A Review," *Engineering Journal*, AISC, Vol. 38, No. 4, pp. 199–203.
- Li, C., Grondin, G.Y., and Driver, R.G. (2007), "Reliability Analysis of Concentrically Loaded Fillet Welded Joints," Structural Engineering Report No. 271, University of Alberta, Canada.
- Liu, J., Sabelli, R., Brockenbrough, R.L., and Fraser, T.P. (2007), "Expected Yield Stress and Tensile Strength Ratios for Determination of Expected Member Capacity in the 2005 AISC Seismic Provisions," *Engineering Journal*, AISC, Vol. 44, No. 1, pp. 15–25.
- Madugula, M.K.S. and Mohan, S. (1988), "Angles in Eccentric Tension," *Journal of Structural Engineering*, ASCE, Vol. 114, No. 10, pp. 2,387–2,396.
- Marsh, C. (1979), "Tear-Out Failure of Bolt Groups," *Journal of the Structural Division*, ASCE, Vol. 105, No. ST10.
- McNeill, N. and Lloyd, A. (2018), "The Use of Digital Image Correlation to Demonstrate Tension Member Behavior in Structural Steel Design," *CSCE Conference Proceedings*, Canadian Society of Civil Engineers, June 13–16.
- Mullin, D.T. and Cheng, J.J.R. (2004), "Ductile Gusset Plates—Tests and Analyses," *Proceedings of the Pacific Structural Steel Conference*, Long Beach, Calif, March 24–27.
- Orbison, J.G., Wagner, M.E., and Fritz, W.P. (1999), "Tension Plane Behavior in Single-Row Bolted Connections Subjected to Block Shear," *Journal of Constructional Steel Research*, Vol. 49, pp. 225–239.
- Pizzuto, D. (2019), "Block Shear Failures in W-Section Tension Members Connected by Bolted Flange Plates," Master's Thesis, Department of Civil Engineering and Applied Mechanics, McGill University, Montreal, Canada.
- Ricles, J.M. and Yura, J.A. (1983), "Strength of Double-Row Bolted-Web Connections," *Journal of Structural Engineering*, ASCE, Vol. 109, No. 1.
- Sankisa, K.K. (1993), "Compressive Resistance and Block Shear Strength of Angles," Master's Thesis, Department of Civil and Environmental Engineering, University of Windsor, Ontario, Canada.
- Schmidt, B.J. and Bartlett, F.M. (2002), "Review of Resistance Factor for Steel: Data Collection," *Canadian Journal of Civil Engineering*, Vol. 29.
- Teh, L.H. and Deierlein, G.G. (2017), "Effective Shear Plane Model for Tearout and Block Shear Failure of Bolted Connections," *Engineering Journal*, AISC, Vol. 54, No. 3, pp. 181–194.
- Tsai, M. (1992), "Reliability Models of Load Testing," PhD Dissertation, University of Illinois at Urbana-Champaign, Urbana, Ill.
- Udagawa, K., and Yamada, T. (1998), "Failure Modes and Ultimate Tensile Strength of Steel Plates Jointed with High-Strength Bolts," *Journal of Structural and Construction Engineering*, Transactions of AIJ, Architectural Institute of Japan, No. 505.
- Wen, H. and Mahmoud, H. (2017), "Simulation of Block Shear Fracture in Bolted Connections," *Journal of Constructional Steel Research*, Vol. 134, pp. 1–16.
- Yam, M.C.H., Grondin, G.Y., Wei, F., and Chung, K.F. (2011), "Design for Block Shear of Coped Beams with a Welded End Connection," *Journal of Structural Engineering*, ASCE, Vol. 137, No. 8.
- Yura, J.A., Birkemoe, P.C., and Ricles, J.M. (1982), "Beam Web Shear Connections: An Experimental Study," *Journal of Structural Engineering*, ASCE, Vol. 108, No. ST2.
- Zeynali, Y., Samimi, M.J., Mazroei, A., Marnani, J.A., and Rohanimanesh, M.S. (2017), "Experimental and Numerical Study of Frictional Effects on Block Shear Fracture of Steel Gusset Plates with Bolted Connections," *Thin-Walled Structures*, Vol. 121.